Highlighting the possibility of parallel mechanism in planar ternary photovoltaic cells

L. Cattin, Z. El Jouad, M. Siad, A. Mohammed Krarroubi, G. Neculqueo, L. Arzel, N. Stephant, M. Mastropasqua Talamo, F. Martinez, M. Addou, et al.

RESEARCH ARTICLE | NOVEMBER 29 2018

Highlighting the possibility of parallel mechanism in planar ternary photovoltaic cells

L. Cattin ✉; Z. El Jouad; M. B. Siad; A. Mohammed Krarroubi; G. Neculqueo; L. Arzel; N. Stephant; M. Mastropasqua Talamo; F. Martinez; M. Addou; A. Khelil; M. Morsli; P. Blanchard; J. C. Bernède

AIP Advances 8, 115329 (2018)
https://doi.org/10.1063/1.5037531

Highlighting the possibility of parallel mechanism in planar ternary photovoltaic cells

L. Cattin,[1,a] Z. El Jouad,[1,2] M. B. Siad,[3,4] A. Mohammed Krarroubi,[3,4] G. Neculqueo,[5] L. Arzel,[1] N. Stephant,[1] M. Mastropasqua Talamo,[6] F. Martinez,[7] M. Addou,[2] A. Khelil,[4] M. Morsli,[8] P. Blanchard,[6] and J. C. Bernède[3]

[1]*Institut des Matériaux Jean Rouxel (IMN), CNRS, UMR 6502, Université de Nantes, 2 Rue de la Houssinière, BP 32229, 44322 Nantes Cedex 3, France*
[2]*Laboratoire Optoélectronique et Physico-Chimie des Matériaux, Université Ibn Tofail, Faculté des Sciences, BP 133, Kenitra 14000, Morocco*
[3]*MOLTECH-Anjou, CNRS, UMR 6200, Université de Nantes, 2 Rue de la Houssinière, BP 92208, Nantes F-44000, France*
[4]*Université d'Oran1—Ahmed Ben Bella, LPCMME, BP 1524 ELM Naouer, 31000 Oran, Algérie*
[5]*Departamento de Materiales Avanzados, Comisión Chilena de Energía Nuclear, Amunátegui 95, Santiago de Chile 8340701, Chile*
[6]*MOLTECH-Anjou, CNRS, UMR 6200, Université d'Angers, 2 Bd Lavoisier, 49045 Angers Cedex, France*
[7]*Departamento de Ciencia de los Materiales, Facultad de Ciencias Físicas y Matemáticas, Universidad de Chile, Casilla 2777, Santiago, Chile*
[8]*Université de Nantes, Faculté des Sciences et des Techniques, 2 Rue de la Houssinière, BP 92208, Nantes F-44000, France*

(Received 25 April 2018; accepted 23 July 2018; published online 29 November 2018)

Ternary and binary planar heterojunctions (PHJs) have been realized and characterized. The outer layers of the active organic layers are pentathiophene (5T) and fullerene (C_{60}), while the intercalated layer is AlPcCl. The binary, 5T/C_{60}, 5T/AlPcCl and ternary 5T/AlPcCl/C_{60} PHJs were characterized by J-V and EQE measurements. The morphology of the organic layers was studied by scanning electron microscopy and atomic force microscopy, while the band structure of 5T was estimated by cyclic voltammetry. The study shows that it is possible to overcome the difficulties linked to the need for the good band matching of the three successive organic layers by using as a first electron donor layer, a layer whose morphology allows the ternary structure to behave as it was two diodes in parallel. Actually, due to this specific morphology the intercalated layer is discontinuous, which allows achieving parallel mechanism in planar ternary photovoltaic cells. This parallel mechanism in the 5T/AlPcCl/C_{60} organic photovoltaic cells (OPVCs) allows achieving efficiency of 1.25%, which represents a 65 % increase by comparison with the best binary 5T/C_{60} OPVC. It means that the morphology of the 5T layer, with its many protrusions and holes, allows ternary OPVCs to behave like parallel-linkage diodes. This behaviour allows the ternary OPVCs to achieve efficiencies higher than those obtained with the binary 5T/C60 OPVCs. https://doi.org/10.1063/1.5037531

I. INTRODUCTION

In the field of solar cells, Organic Photovoltaic Cells (OPVCs) can become complementary to those in silicon due to their advantage of lightweight, flexibility and material diversity.[1] The active layer of OPVCs consists in an organic couple electron donor/electron acceptor (ED/EA) either in

[a]Corresponding author: Linda CATTIN E-Mail: Linda.Cattin-Guenadez@univ-nantes.fr

TABLE I. Variation of the parameters of OPVCs based on the binary structure 5T/AlPcCl with the thickness of the AlPcCl layer.

Films thickness (nm)					
5T	AlPcCl	Voc (V)	Jsc (mA/cm^2)	FF (%)	η (%)
70	20	0.38	2.94	38	0.42
70	22	0.40	2.95	39	0.46
70	24	0.40	2.45	37.5	0.36

the form of bulk heterojunction (BHJ) or planar heterojunction (PHJ).[2] Power conversion efficiency (PCE) of OPVCs is continuously improved through the synthesis of new ED[3] and, during the last years, new EA.[4,5]

However the PCE is limited by the narrow absorption spectra of the organic materials. In order to widen the absorption range of the OPVCs it is possible to use new device architectures employing three molecular species,[6] two ED and one EA[7] or one ED and two EA.[8] The absorption spectra of at least two of these organic layers must be complementary in order to widen effectively the absorption range of the OPVCs. For instance, significant increase in PCE by employing one ED and two EA in PHJ has been already obtained.[8]

If it is interesting to develop high-performance products, it is important to keep in mind that another important criterion is the ease to synthesize the molecules. Syntheses of thiophene derivatives are well known and these materials are usually stable, therefore we have chosen pentathiophene (5T) as electron donor.[9] In the present work we used PHJ deposited under vacuum by sublimation of small organic molecules due to the fact that the organic materials we have chosen to test are insoluble small molecules i.e. pentathiophene (5T), chloro-aluminum phthalocyanine (AlPcCl) and fullerene (C_{60}). Moreover, the sublimation process provides an additional purification step for the small molecules.[10]

We have already shown that binary OPVC based on the couple 5T/C_{60} achieves significant PCE. However the maximum PCE of these OPVCs was limited by its small open circuit voltage value (Voc = 0.41 V).[11] The maximum value of the open circuit voltage, Voc, follows the energy difference between lowest unoccupied molecular orbital (LUMO) of EA and the highest occupied molecular orbital (HOMO) of ED.[12] It means that the maximum theoretical value of Voc, is 1.25 V in the case of 5T/C_{60} (Table I), which shows that there is a quite large difference between the maximal theoretical value and the experimental value. Such large energy loss is usually attributed to bad interface properties inducing high recombination rate.[13] Therefore it could be interesting to introduce an intermediate layer which not only has a complementary absorption band to widen the absorption window, but also possesses appropriate interface properties with both others organic layers to reduce the energy loss. For instance, if two EDs used with C_{60} acceptor give two different Voc, one for each ED, it was shown that the Voc of the ternary OPVC using these two EDs and C_{60} is intermediate between the two Voc obtained with the binary OPVCs. In such structures, the second ED, intercalated between the first ED and the EA must be very thin, like a buffer layer.[14–16]

In the present work, in order to try to improve the efficiency of the OPVCs using 5T as ED we inserted between 5T and C_{60}, AlPcCl, as second ED. AlPcCl is an efficient ED in binary OPVCs using C_{60} as EA, with a Voc value of 0.7 V.[17] Therefore, in the present work, we used three organic materials, 5T, AlPcCl, and C_{60} to grow ternary OPVCs. We show that if the band structure of the materials used is determinant for the OPVC performance, others parameters, such as surface roughness of the bottom ED, are also very important.

II. EXPERIMENTAL

A. Organic molecules

The active molecules AlPcCl, C_{60} and also AlQ_3, CuI and MoO_3, which were used as buffer layers in the OPVCs were provided by CODEX-International (France) while 5T, was synthesized in the Chilean laboratory involved in this work.

B. Organic photovoltaic cells deposition process and characterization

After cleaning with soap, the ITO coated glass substrates were rinsed in running deionised water. Then the substrates were dried with an argon flow and loaded into a vacuum chamber (10^{-4} Pa). The organic active layers were sandwiched between two electrodes, a transparent ITO anode and an Al cathode. Moreover, hole and electron extracting layers are inserted between the electrodes and the organic active layer. These layers allow selective carriers extraction. The hole extracting layer (HEL) inserted between the ITO anode and ED was a double layer MoO_3/CuI.[18,19] The HEL improves the hole collection while it blocks the electrons. The electron extracting layers, which must block holes and facilitate electron extraction, was a Tris-(8-hydroxyquinoline) Aluminium (Alq_3) layer.[20] More precisely, this layer was called exciton blocking layer (EBL) in the case of PHJ, because it blocks exciton transport towards the cathode. It also protects C_{60} from metallic ion contamination during the cathode deposition.[21]

All the layers were deposited in a vacuum of 10^{-4} Pa. The thin film deposition rates and thicknesses were measured *in situ* with a quartz monitor.

Following our earlier studies,[22] the deposition rate and final thickness were 0.05 nm/s and 3 nm for MoO_3, 0.005 nm/s and 1.5 nm for CuI, 0.05 nm/s, 40 nm for C_{60} and 0.1 nm/s, 9 nm for Alq_3. The effect of the thickness of the AlPcCl and 5T films on the solar cell performances was studied during the present work.

After organic thin film deposition, the aluminium top electrodes were thermally evaporated, without breaking the vacuum, through a mask with 2 mm x 8 mm active areas.

The structures used were as follow:

Glass/ITO(100nm)/MoO_3(3nm)/CuI(1.5nm)/organic active layers/Alq_3(9nm)/Al(120nm), the different configurations of the organic active layers are described in the next paragraph.

Electrical characterizations were performed with an automated I-V tester, in the dark and under sun global AM 1.5 simulated solar illumination. Performances of photovoltaic cells were measured using a calibrated solar simulator (Oriel 300W) at 100 mW/cm^2 light intensity adjusted with a PV reference cell (0.5 cm^2 CIGS solar cell, calibrated at NREL, USA). Measurements were performed at an ambient atmosphere. All devices were illuminated through TCO electrodes.

In order to check the contribution of the different organic layers to the generated current, we also measured the External Quantum efficiency (EQE) of the different OPVCs. EQE was measured on apparatus built up in our laboratory. The measurements of incident photon-to-current conversion efficiency are done with monochromatic continuous light without modulation. The measurement duration for a given wavelength was long enough to reach a steady-state value and to minimize noise.

C. Complementary characterizations

Optical transmission spectra were recorded using Cary spectrophotometer. The optical absorption has been measured at wavelengths of 1 to 0.35 λm.

In PHJ, it is known that an increase of the surface roughness of the bottom layer increases the ED/EA interface area which improves the charge separation efficiency and therefore Jsc. However, such increase of the surface roughness may induce leakage current, which results in a deterioration of FF and Voc. A trade off between these two effects must be found and it is important to check the morphology of the bottom layer in PHJ. Therefore, parallel to the study of the electrical and optical properties of the OPVCs, we realized a morphological study of various layers constituting them.

The morphology of the layers was observed by scanning electron microscopy (SEM) and atomic force microscopy (AFM). The surface and layer cross sections were observed through scanning electron microscopy with a JEOL 6400F ("Centre de microcaractéristion, Institut des Matériaux Jean Rouxel, Université de Nantes").

AFM images of the films were taken ex-situ at atmospheric pressure and room temperature. All measurements have been performed in intermittent contact mode (Nanosurf Easyscan 2 AFM). The root mean square (RMS) roughness given in the following has been calculated by averaging the roughness obtained from each images for a given sample.

The HOMO and LUMO of pentathiophene were evaluated using cyclic voltammetry. A three electrodes cell configuration with Pt as the counter electrode is used for this work. Experiments

were carried out in one-compartment cell equipped with platinum electrodes and a saturated calomel reference electrode (SCE) using a Biologic SP-150 potentiostat with positive feedback compensation. The working electrode (here a Pt disk of 2 mm diameter was coated with a 50 nm thick layer of vacuum-deposited pentathiophene), dipped in an electrolyte solution (0.1 M tetra-butylammonium hexafluorophosphate -$TBAPF_6$ in acetonitrile), is biased with respect to the reference electrode, the scan rate being 100 mV/s. The onset of oxidation ($E_{ox,onset}$) and reduction potentials ($E_{red,onset}$) were measured at + 0.55 V and – 1.93 V *vs* the ferrocenium/ferrocene couple, respectively. The HOMO and LUMO energy levels are calculated from the following equations.[23]

$$\text{HOMO} = \text{Ionization Potential} = -(E_{ox,onset}\ vs\ Fc^{+}/Fc + 5.1)\ \text{eV}$$

$$\text{LUMO} = \text{Electron Affinity} = -(E_{red,onset}\ vs\ Fc^{+}/Fc + 5.1)\ \text{eV},$$

III. EXPERIMENTAL RESULTS

We have shown in an earlier publication,[11] that the best PV performance obtained with the binary OPVC based on the couple $5T/C_{60}$ was PCE = 0.81%, with Voc = 0.40 V, Jsc = 3.64 mA/cm2 and FF = 56%, the thickness of the 5T layer being 70 nm. In order to verify if the interfaces used within the ternary structures $5T/AlPcCl/C_{60}$ were all active, we also fabricated 5T/AlPcCl binary PHJ.

Before starting the electrical study of the different OPVCs configurations we recorded the absorption spectrum of the different active layers used. We can see in Figure 1 that the absorption spectrum of 5T is complementary to that of AlPcCl.

A. Electrical characterization of the different OPVCs

After measuring the optical properties of the different organic active layers, we realized the different OPVCs configurations using these layers and checked their electrical properties. These configurations were based either on the binary structures $5T/C_{60}$, 5T/AlPcCl or the ternary structure $5T/AlPcCl/C_{60}$.

Before growing ternary structures, we began with 5T/AlPcCl bilayer PHJ. The hole mobility in 5T being relatively high,[24] while the electron mobility in AlPcCl is smaller than that in C_{60}, we choose to start with the optimum thickness of 5T encountered in the couple $5T/C_{60}$, while we added a quite thin film of AlPcCl.

Results obtained with a typical 5T/AlPcCl structure are reported in Table I. The PCE saturates at 0.46% for a thickness of AlPcCl of 20 nm. All the OPVC parameters are small. It is clear, from the J-V characteristics of the 5T/AlPcCl structure in Figure 2 that the diode quality of this couple is poor. To check this hypothesis we have measured the EQE of the 5T/AlPcCl OPVC. As shown, in Figure 3, the shape of the EQE spectrum does not follow that of the optical density. The EQE curve of the OPVC exhibits a main photo-response from 340 nm to 500 nm. Then, a second low intensity domain

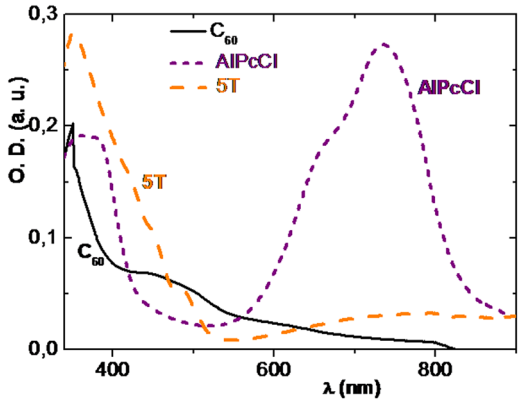

FIG. 1. Absorption spectra of 5T (– – –), AlPcCl (– · – · – · –) and C_{60} (–).

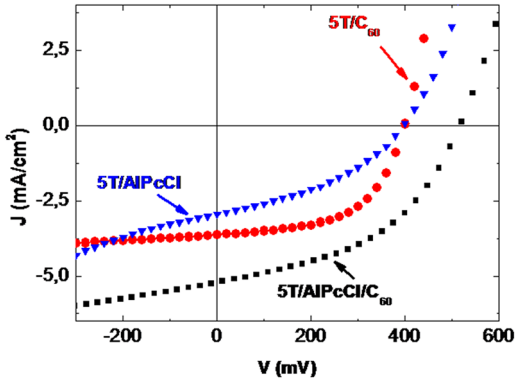

FIG. 2. J-V characteristics of the OPVCs for each probed device configuration: (▼) 5T/AlPcCl; (●) 5T/C_{60}; (■) 5T/AlPcCl/C_{60}.

is visible between 600 and 800 nm. Therefore, unlike what is generally observed, the general shape of the EQE spectrum is not consistent with the corresponding absorption spectra, the absorption curve of the bilayer 5T/AlPcCl being the sum of the absorption of each component. The EQE curve shows that a large majority of created carriers are from the 5T layer, while the contribution of AlPcCl is very small. Actually, it can be seen from the energy level diagram (Inset figure 3), that the excitons created in AlPcCl cannot dissociate at the 5T interface. As such, only a significant photocurrent from 5T is expected. A different IQE for each material and wavelength dependent IQE has been reported before.[25,26]

Nevertheless, as said above, in the light of earliest studies,[14–16] the idea was to use AlPcCl as a "buffer layer" at the interface 5T/C_{60}, to improve Voc, so we have inserted a very thin AlPcCl layer between the 5T and C_{60} layers.

When a very thin (5 nm, 2.5 nm) AlPcCl layer is used, the results obtained with the 5T/AlPc/C_{60} structures, were highly disappointing (Table II).

The addition of a 2.5 nm thick AlPcCl interlayer increases Jsc from 3.64 to 3.80 mA/cm^2, representing a 6.6 % increase over the 5T/C_{60} device. Nevertheless this quite small increase of Jsc was counterbalanced by the decrease of FF, from 56% to 50%, while the expected positive effect on the Voc value was not effective. Similar unsuccessful result was obtained with 5 nm of AlPcCl (Table II). Therefore, we proceeded to a progressive increase of the thickness of the AlPcCl layer, while decreasing that of 5T to prevent the cell from becoming too resistant, and the efficiency of the OPVCs was significantly improved. For example, with 50 nm of 5T and 10 nm of AlPcCl a significant improvement Jsc and Voc was obtained while FF continues to decrease. All of these changes result in an OPVC efficiency of 0.98%, *i.e.* higher than that of the best 5T/C_{60} binary OPVC. Consequently

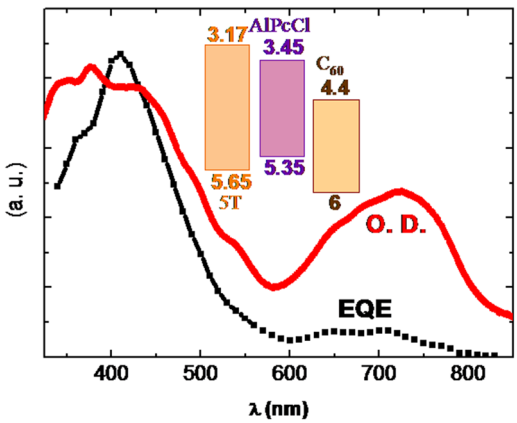

FIG. 3. EQE (■) and optical density (—) spectra of OPVC with a binary structure 5T/AlPcCl.

TABLE II. Variation of the parameters of OPVCs based on the ternary structure 5T/AlPcCl/C_{60} with the thickness of the organic layers.

Sample (thickness nm)						
5T	AlPcCl	C60	Voc (V)	Jsc (A/cm^2)	FF (%)	η (%)
70	-	40	0.40	3.64	56	0.81
60	2.5	40	0.38	3.80	50	0.72
60	5	40	0.41	3.88	47	0.73
50	10	40	0.50	4.89	40	0.98
50	15	40	0.50	5.16	40	1.02
50	18	40	0.50	4.99	39	0.97
60	10	40	0.52	5.21	46	1.25
60	15	40	0.46	4.92	45	1.01
60	18	40	0.45	4.86	44	0.96
70	10	40	0.48	5.55	45	1.20
70	15	40	0.47	5.49	43	1.11
70	18	25	0.45	4.32	36	0.7

we increased more the AlPcCl layer thickness. It can be seen in Table II that, with 50 nm of 5T, the maximum efficiency saturate around 1%. For AlPcCl thickness higher than 15 nm, Jsc and η start to decrease. The carrier mobility in 5T being far higher than that of AlPcCl, we proceeded to new experiment using thicker 5T layer and thinner AlPcCl layer. With 60 nm of 5T, the optimum AlPcCl layer is 10 nm, Jsc being significantly improved, an efficiency of 1.25% is reached. Following this success, a thickness of 70 nm of 5T was probed. Here also the optimum AlPcCl thickness is 10 nm, but the optimum efficiency achieved does not over pass that obtained with 60 nm of 5T.

It can be seen in Figure 2 that, in ternary OPVCs the results show enhanced short circuit current density (Jsc), which can be due to broader spectral responses, while, as often encountered, the ternary OPVCs have poorer FF values than binary 5T/C_{60} OPVCs.

To pursue our study, we have measured the EQE of the ternary OPVCs. Here also, EQE measurements integration over the solar spectrum gives J_{EQE} values in good agreement with Jsc deduced from J-V characteristics. In Figure 4, in addition to the EQE spectrum of the binary OPVC, we have represented those of the ternary OPVC for 2 specific thicknesses. Actually, the maximum efficiency is achieved for an AlPcCl thickness of 10 nm, while a significant decrease was measured for 18 nm (Table II). Therefore we choose these two specific thicknesses to deepen the characterizations.

In can be seen in Figure 4, that while the EQE spectrum of the OPVC based on the binary structure 5T/AlPcCl exhibits only one photo-response range, the EQE spectra of the ternary structures exhibit two photo-responses domains. The first is situated in the small wavelength domain and the second between 600 and 800 nm. While the shape of the second domain is similar whatever the intercalated

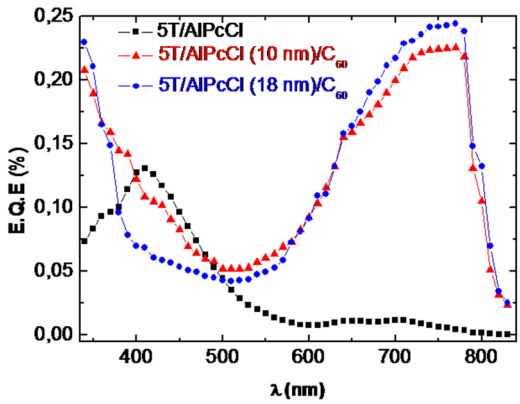

FIG. 4. EQE density spectra of OPVCs with binary and ternary structures: (■) 5T/AlPcCl; (▲) 5T/AlPcCl (10 nm)/C_{60}; (●) 5T/AlPcCl (18 nm)/C_{60}.

layer thickness is, the width of the first domain varies with the thickness of the AlPcCl intercalated layer. For an AlPcCl layer thick of 18 nm it is situated between 340 and 400 nm, whereas, when the AlPcCl layer is thick of only 10 nm, it is situated between 340 and 500 nm. The photo-response in the 600 - 800 nm range corresponds to the contribution of AlPcCl. If we refer to the absorption curves of Figure 1, the absorption in the 340 - 500 nm range, may correspond to three contributions, 5T, C_{60}[26] and, below 420 nm, to AlPcCl. When the AlPcCl layer is thick of 18 nm, the signal, which is situated in a narrower range, *i.e.* 340-400 nm, must be mainly attributed to AlPcCL and C_{60}. However, when this film is thick of 10 nm, the broader part of the signal must be attributed to 5T. In order to try to understand the effect of the AlPcCl layer thickness on the EQE spectrum, we proceeded to a morphological study of the electron donor layers.[27]

To summarise the electrical characterization of the different OPVC configurations, it must be highlighted that the optimum OPVC efficiency, $\eta = 1.25\%$, with Voc = 0.52 V, Jsc = 5.21 mA/cm^2, FF = 46%, was obtained with the ternary structure 5T (60 nm)/AlPcCl (10 nm)/C_{60} (40 nm). It means that we were able to increase by more than 60% the efficiency of the starting 5T/C_{60} binary structure.

B. Morphological study of the organic active layers

The 5T layer being the bottom layer of the organic semiconductors present in the structures, we have first studied its morphology by SEM and AFM. In Figure 5 its surface visualization shows that clearly shaped grains are visible. If most of them are parallel to the plane of the substrate, some of them make an angle close to 90 ° with the substrate. By tilting the sample and using a lower magnification, it can be demonstrated that these protrusions are present all over the layer (Figure 5b).

This observation is corroborated by the cross section shown in Figure 6b where protrusions perpendicular to the plan of the substrate are clearly visible. It must be noted that not only protrusions, but also holes, starting from the bottom electrode, are visible.

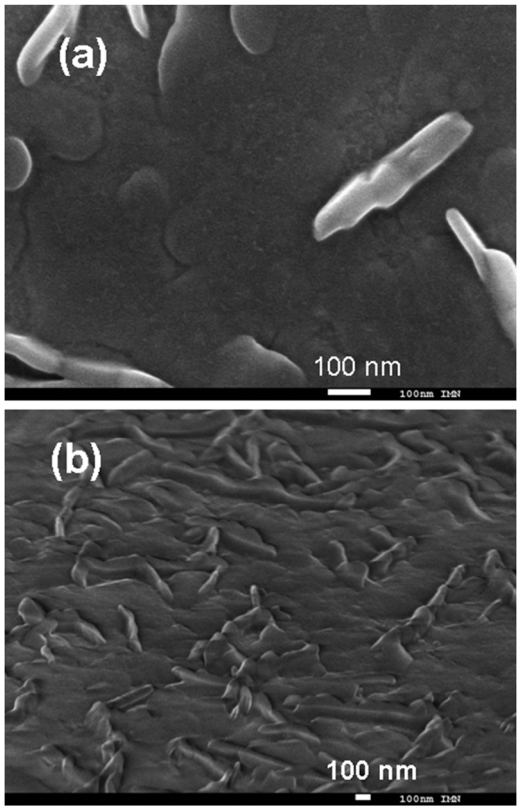

FIG. 5. Surface visualization of a 5T layer (Thickness measured by the quartz monitor: 60 nm): (a) sample horizontal; (b) sample tilted of 15°.

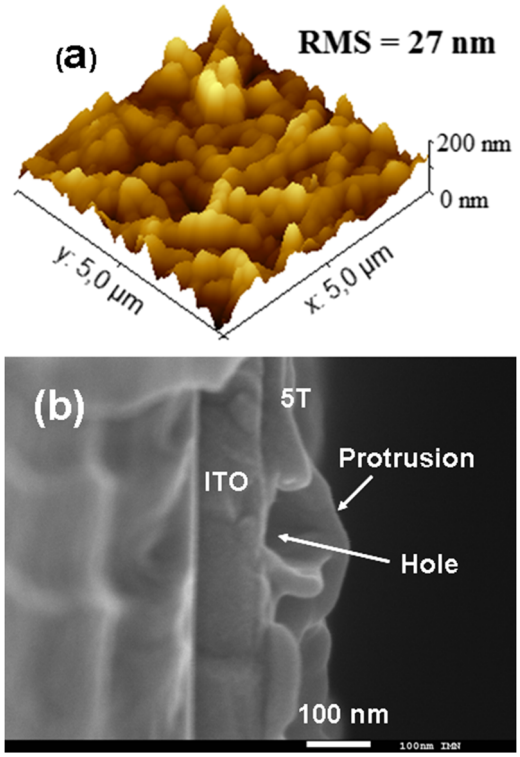

FIG. 6. 5T layer (Thickness measured by the quartz monitor: 60 nm), (a) AFM image, in 3D and (b) Cross section visualization of a structure Glass/ITO/MoO_3/CuI/5T.

The surface roughness of the 5T layers appearing high, it has been quantified by AFM. The 3D AFM image shown in Figure 6a confirms high surface roughness and the RMS roughness deduced is 27 nm, while the maximum peak-to-peak value was 135 nm.

After the morphological study of the 5T layer we proceeded to the deposition and visualization of the second organic layer. Therefore we proceeded to the morphological study of the optimum structures deduced from Table II: ITO/MoO_3/CuI/5T (60 nm)/AlPcCl (10 nm).

Also for comparison, we studied a structure which exhibits typically smaller performances ITO/MoO_3/CuI/5T (60 nm)/AlPcCl (18 nm). The cross sections of the ITO/MoO_3/CuI/5T (60 nm)/AlPcCl (x nm) structure with either 18 nm (Figure 7a) or 10 nm (Figure 7b) are visible as insets of Figure 7, while the surfaces of these structures are shown in Figure 7. It can be seen quite clearly in these sections that, while when the AlPcCl layer is thick of 18 nm it covers quite well the 5T film and its protrusions (Inset Figure 7a). When the AlPcCl layer is only 10 nm, some 5T protrusions are not covered (Figure 7b). If the surface visualizations of Figure 7 confirm these tendencies, they allow us to see more clearly the dependence of the surface coverage of the 5T bottom layer with the AlPcCl layer thickness. When the AlPcCl layer is thick of 18 nm, it covers nearly the whole surface of the 5T layer, even if some small holes are still present. It is remarkable that the 5T protrusions themselves are covered. When the AlPcCl layer is thick of only 10 nm, it is clearly not continuous and therefore it covers only partly the 5T layer. Here, the protrusions are not covered.

For 5T, due to the wide range of values of HOMO-LUMO given in the literature,[11,24,28,29] we prefer to re-measure these values using cyclic voltammetry. The LUMO and HOMO values, calculated as explained in the experimental paragraph, are, in absolute values, 3.17 eV and 5.65 eV respectively. These values confirm that 5T can be a good ED. The difference LUMO-HOMO leads to an estimation of the energy gap of the material E_g of 2.48 eV. It must be noted that the validity of the cyclic voltammetry study is corroborated by the fact that this gap value is in good agreement with the value deduced from the optical absorption spectra of 5T film (100 nm thick), since this value is 2.38 eV (Figure 1). These HOMO and LUMO values will be will be discussed below.

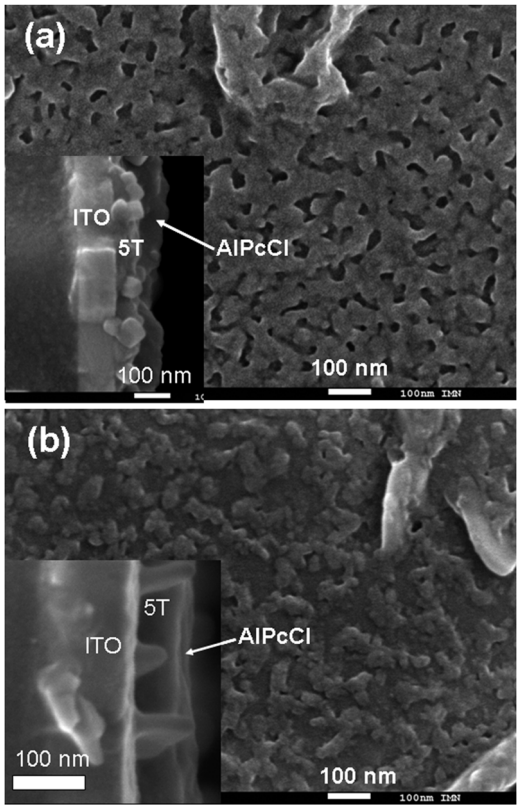

FIG. 7. Surface visualization of structures Glass/ITO/MoO_3/CuI/5T (60 nm)/AlPcCl, the AlPcCl thickness being (a) 20 nm and (b) 10 nm. Inset Figure 7: Corresponding cross sections.

IV. DISCUSSION

The values of the HOMO and LUMO of AlPcCl and C_{60} being known, and following the values measured for 5T, a summary of these values is given in Table III and the representation of the corresponding band scheme is shown in the Inset of Figure 3.

About the interface band matching between 5T and AlPcCl, the cyclic voltammetric study shows that, if the value of $\Delta(LUMO_A\text{-}LUMO_D) = 0.28$ eV is sufficient and may allow the photo-induced electron transfer from 5T to AlPcCl, the $\Delta(HOMO_A\text{-}HOMO_D)$ value is negative, suggesting that these 5T/AlPcCl interface is not favourable for hole extraction (Inset figure3). The use of a thin layer of AlPcCl (1-5 nm) as a buffer layer for an effective tunnel effect having given disappointing results, we worked with thicker AlPcCl layers.

In front of such difficulties together with the objective to check the efficiency of all the organic interfaces present in our ternary structures, we studied 5T/AlPcCl binary OPVCs. We will first discuss the behaviour of these binary structures. The unfavourable band scheme of these structures not only limits the hole extraction efficiency and therefore Jsc and FF, but also Voc. This unfavourable effect is well put in evidence by the EQE measurements of Figure 3. The very small current measured between 600 and 800 nm, shows that, despite the high absorption value of AlPcCl, its contribution to the current is very small. This bad result, is due to the fact that $\Delta(HOMO_A\text{-}HOMO_D)$ is negative,

TABLE III. HOMO and LUMO values of the different organic molecules used.

Organic molecule	5T	AlPcCl	C_{60}
LUMO	3.17	3.45	4.4
HOMO	5.65	5.35	6

which impedes hole transfer from AlPcCl to 5T and therefore the collection of hole issued from the excitons created in the AlPcCl layer. On the contrary the LUMO offset allows efficient electron transfer from 5T to AlPcCl.

Therefore, such bad band alignment should be also seriously unfavourable for the 5T/AlPcCl/C_{60} ternary OPVC. Surprisingly, the results obtained are encouraging, since, by comparison with the initial 5T/C_{60} binary OPVC, the efficiency of the ternary structure is increased by 65%. Such improvement will be discussed in the light of the different characterization studies presented above. The evolution of the shape of the EQE spectra with the thickness of AlPcCl is very informative on the behaviour of the ternary structures. When the AlPcCl layer thickness increases from 10 to 18 nm, the contribution of the different organic layers to the carrier creation, changes significantly (Figure 4). For 10 nm of AlPcCl, the three layers contribute to charge carrier formation. As discussed in paragraph 3, the main contribution is due to AlPcCl, but the 5T contribution is significant, while that of C_{60} is smaller due to the well known fact that C_{60} absorbs faintly the light. When the AlPcCl layer thickness increases up to 18 nm, the shape of the EQE spectrum is significantly modified due to the fact that the contribution of 5T to carrier formation has strongly decreased as testified by the narrowing of the EQE signal in the short wavelength range (Figure 4).

The morphological study of the different structures is very helpful to explain the variation of the OPVC performances, J-V characteristics and EQE spectrum, with the AlPcCl thickness. As shown in the Figures 5 and 6, the surface of the 5T layer is quite rough with holes and protrusions all over the layer. When such rough layer is covered by a thin film, the coverage of the bottom layer depends on the thickness of this top layer. This fact is clearly visible in Figure 7. While, when 18 nm of AlPcCl are deposited onto the 5T layer, even the protrusions are covered, a large part of the 5T layer is not covered by the 10 nm thick film. These different behaviours are schematized in Figure 8. The 5T layers are rough due to the presence of protrusions and holes and the covering efficiency of AlPcCl layer depends on its thickness. It means that, as schematized in Figure 8, in the case of an AlPcCl layer of 10 nm, the intermediate layer is discontinuous (Figure 7b) and the C_{60} film is not only directly in contact with AlPcCl, but also with 5T. Therefore the ternary structure behaves as if it was constituted of independent parallel binary structures: anode/5T/C_{60}/cathode and anode/AlPcCl/C_{60}/cathode binary structures. Such parallel binary structures are independent of the bad 5T/AlPcCl band alignment. Both EDs, 5T and AlPcCl contributes to the current as testified by the EQE spectrum. Therefore, when the AlPcCl layer is thick of only 10 nm this results in, not only AlPcCl/C_{60} interface, but also in direct contact 5T/C_{60} which makes possible dissociation mechanism for excitons issued from both EDs (Figure 8a). Such possibility circumvent the unfavourable negative

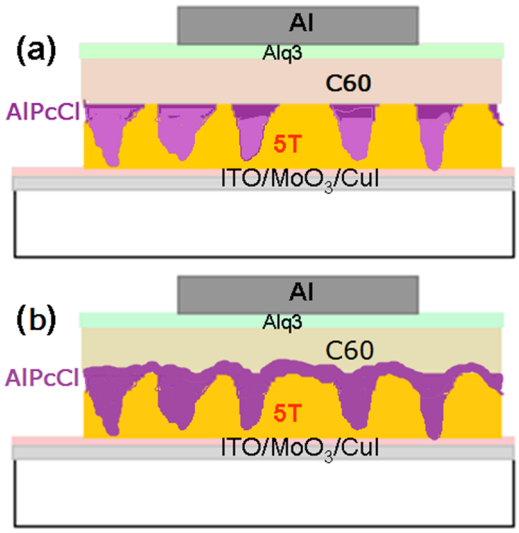

FIG. 8. Schematization of the geometrical section of PHJs with different intercalated AlPcCl layer thickness: (a) 10 nm, (b) 18 nm.

value of $\Delta(HOMO_A\text{-}HOMO_D)$. The excitons created in 5T being in direct contact with $5T/C_{60}$ interface, while those from AlPcCl also can diffuse toward $AlPcCl/C_{60}$ interfaces. By analogy with the ternary bulk-heterojunction (BHJ), when the AlPcCl is thick of only 10 nm, the behaviour of the ternary PHJ $5T/AlPcCl/C_{60}$ is based on a process similar to the parallel-linkage mechanism of ternary BHJ.[7,30] Such mechanism neither requires accurate band matching between the two EDs, nor energy transfer. Here, excitons generated in each ED migrates towards ED/C_{60} interface and then dissociate into free electrons and holes.[7] These generated holes are transported through their corresponding donor channels to the anode and the electrons transport via acceptor layer to the cathode as in normal binary solar cells. About the Voc, in parallel-linkage ternary OPVCs its value is between the values measured for the individual "sub-cells", which is in good agreement with the Voc value we measured, 0.52 V, higher than the value measured for $5T/C_{60}$, but smaller than that expected for $AlPcCl/C_{60}$, 0.7 V.

When the AlPcCl layer thickness increases to 18 nm it covers nearly all the bottom layers, prohibiting direct $5T/C_{60}$ contact, which makes that the 5T contribution is significantly reduced due to unfavorable band structure of the ternary OPVC. Holes formed on AlPcCl molecules cannot hop to 5T molecules, due to the mismatch in the donor's energy levels. 5T acts as a blocking layer, restricting hole transport from AlPcCl to the anode. The HOMO offset between 5T and AlPcCl limits the charge transport and ultimately degrades ternary OPVCs performances.

However, due to the hole present in the 5T layer, some anode/$AlPcCl/C_{60}$/cathode binary structures are still present as visible in the scheme of Figure 8b and the OPVC efficiency, if smaller than that obtained with 10 nm of AlPcCl, is still better than that obtained with $5T/C_{60}$ binary diodes.

It must be noted that, even if the introduction of a thin (10 nm) of AlPcCl between 5T and C_{60} permits an increase by more than 60% of the efficiency of the starting $5T/C_{60}$ binary structure, it stays smaller than the maximum efficiency obtained with the binary OPVC $AlPcCL/C_{60}$ (3.97%).[17] Nevertheless, all these results show that the choice of a first donor whose thin layers have a morphology close to that of 5T, but whose optical properties would be more complementary to those of AlPcCl, should allow to obtain a yield worthy of interest.

V. CONCLUSION

Through the study of ternary OPVCs we show that if the band structure is decisive, the morphology of the organic layers is also critical. For optimum efficiency, the cascade structure must be respected. However, the cyclic voltammetric study of 5T leading to HOMO and LUMO levels, shows that it is not the case when it is associated with AlPcCl since at the interface 5T/AlPcCl we have $\Delta(HOMO_A\text{-}HOMO_D) < 0$. As a consequence for the ternary structure $5T/AlPcCl/C_{60}$, when the intermediate AlPcCl layer completely recovers the 5T bottom layer, the OPVC efficiency is small, due to the high recombination rate and poor carrier collection efficiency induced by the bad band matching. The study of the influence of the AlPcCl thickness on the ternary OPVCs performances shows that it is possible to, at least partially, overpass this difficulty by using sufficiently thin intermediate AlPcCl layer in order to only partly recover the bottom 5T layer. In that case, the morphology of the 5T layer, with its many protrusions and holes, allows ternary OPVCs to behave like parallel-linkage mechanism of ternary BHJ, hence achieving efficiencies higher by 60% than that obtained with the binary $5T/C_{60}$ OPVC.

ACKNOWLEDGMENTS

The authors would like to thanks CNRST (PPR/2015/9 - Ministère, Morocco) for its financial support.

[1] M. Finn III, C. J. Martens, A. V. Zaretski, B. Roth, R. R. Søndergaard, F. C. Krebs, and D. J. Lipomi, "Mechanical stability of roll-to-roll printed solar cells under cyclic bending and torsion," Sol. Energy Mater. Sol. Cells **174**, 7–15 (2018).
[2] J. C. Bernède, "Organic photovoltaic cells: History, principle and techniques," Journal of The Chilean Chemical Society **53**, 1549–1564 (2008).
[3] S. O. Oseni and G. T. Mola, "Properties of functional layers in inverted thin film organic solar cells," Sol. Energy Mater. Sol. Cells **160**, 241–256 (2017).
[4] J. Hou, O. Inganäs, R. H. Friend, and F. Gao, "Organic solar cells based on non-fullerene acceptors," Nature Materials **17**, 119–128 (2018).

[5] D. Baran, T. Kirchartz, S. Wheeler, S. Dimitrov, M. Abdelsamie, J. Gorman, R. S. Ashraf, S. Holliday, A. Wadsworth, N. Gasparini, P. Kaienburg, H. Yan, A. Amassian, C. J. Brabec, J. R. Durrant, and I. McCulloch, "Reduced voltage losses yield 10% efficient fullerene free organic solar cells with >1 V open circuit voltages," Energy Environ. Sci. **9**, 3783–3793 (2016).
[6] A. Barito, M. E. Sykes, B. Huang, D. Bilby, B. Frieberg, J. Kim, P. F. Green, and M. Shtein, "Universal design principles for cascade heterojunction solar cells with high fill factors and internal quantum efficiencies approaching 100%," Adv. Energy Mater. **4**, 1400216 (2014).
[7] Q. An, F. Zhang, J. Zhang, W. Tang, Z. Deng, and B. Hu, "Versatile ternary organic solar cells: A critical review," Energy Environ. Sci. **9**, 281–322 (2016).
[8] K. Cnops, B. P. Rand, D. Cheyns, B. Verreet, M. A. Empl, and P. Heremans, "8.4% efficient fullerene-free organic solar cells exploiting long-range exciton energy transfer," Nature Communications **5**, 3406 (2014).
[9] A. Mishra and P. Bâuerle, "Small molecule organic semiconductors on the move: Promises for future solar energy technology," Angew. Chem., Int. Ed. **51**, 2020–2067 (2012).
[10] K.-W. Chen, C.-W. Huang, S.-Y. Lin, Y.-H. Liu, T. Chatterjee, W.-Y. Hung, S.-W. liu, and K.-T. Wong, "Merocyanines for vacuum-deposited small molecule organic solar cells," Org. Electron. **26**, 319–326 (2015).
[11] Z. El Jouad, L. Cattin, F. Martinez, G. Neculqueo, G. Louarn, M. Addou, P. Predeep, J. Manuvel, and J. C. Bernède, "Improvement of pentathiophene/fullerene planar heterojunction photovoltaic cells by improving the organic films morphology through the anode buffer bilayer," Eur. Phys. J. Appl. Phys. **74**, 24603 (2016).
[12] M. Vogel, S. Doka, Ch. Breyer, M. Ch. Lux-Steiner, and K. Fostiropoulos, "On the function of a bathocuproine buffer layer in organic photovoltaic cells," Appl. Phys. Lett. **89**, 163501 (2006).
[13] J. Benduhn, K. Tvingstedt, F. Piersimoni, S. Ullbrich, Y. Fan, M. Tropiano, K. A. Mc Garry, O. Zeika, M. K. Riede, C. J. Douglas, S. Barlow, and S. R. Marder, "Intrinsic non-radiative voltage losses in fullerene-based organic solar cells," Nature Energy **2**, 17053 (2017).
[14] A. P. Yen, A.-M. Hor, J. S. Preston, R. Klenker, N. M. Bamsey, and R. O. Loutfy, "A simple parallel tandem organic solar cell based on metallophthalocyanines," Appl. Phys.Lett. **98**, 173301 (2011).
[15] Z. R. Hong, R. Lessmann, B. Maenning, Q. Huang, K. Harada, M. Riede, and K. Leo, "Antenna effects and improved efficiency in multiple heterojunction photovoltaic cells based on pentacene, zinc phthalocyanine, and C_{60}," J. Appl. Phys. **106**, 064511 (2009).
[16] Y. Kinoshita, T. Hasobe, and H. Murata, "Control of open circuit voltage in organic photovoltaic cells by inserting an ultrathin metal-phthalocyanine layer," Appl. Phys. Lett. **91**, 083518 (2007).
[17] A. Mohammed-Krarroubi, M. Morsli, A. Khelil, L. Cattin, L. Barkat, S. Tuo, Z. El Jouad, G. Louarn, M. Ghamnia, M. Addou, and J. C. Bernède, "The influence of deposition rates on properties of AlPcCl thin films and on the performance of planar organic solar cells," Phys. Stat. Sol. A **214**, 1700364 (2017).
[18] J. C. Bernède, L. Cattin, M. Makha, V. Jeux, P. Leriche, J. Roncali, V. Froger, M. Morsli, and M. Addou, "MoO_3/CuI hybrid buffer layer for the optimization of organic solar cells based on a donor–acceptor triphenylamine," Sol. Energy Mater. Sol. Cells **110**, 107–114 (2013).
[19] J. Christian Bernède, L. Cattin, and M. Morsli, "About MoO_3 as buffer layer in organic optoelectronic devices," Technology Letters **1**(2), 5–17 (2014).
[20] Y. Lare, B. Kouskoussa, K. Benchouk, S. Ouro Djobo, L. Cattin, F. R. Diaz, M. Gacitua, T. Abachi, M. A. del Valle, F. Amijo, G. A. East, and J. C. Bernède, "Influence of the exciton blocking layer on the stability of layered organic solar cells," J. Phys. Chem. Solids **72**, 97–103 (2011).
[21] X. P. Peumans, V. Bulovic, and S. R. Forrest, "Efficient photon harvesting at high optical intensities in ultrathin organic double-heterostructure photovoltaic diodes," Appl. Phys. Lett. **76**, 2650–2652 (2000).
[22] M. Makha, L. Cattin, S. Dabos-Seignon, E. Arca, J. Velez, N. Stephant, M. Morsli, M. Addou, and J. C. Bernède, "Study of CuI thin films properties for application as anode buffer layer in organic solar cells," Indian Journal of Pure & Applied Physics **51**, 569–582 (2013).
[23] C. M. Cardona, W. Li, A. E. Keifer, D. Stockdale, and G. C. Bazan, "Electrochemical considerations for determining absolute Frontier orbital energy levels of conjugated polymers for solar cell applications," Adv. Mater. **23**, 2367–2371 (2011).
[24] Z. Bao and J. Locklein, *Organic Field Effect Transistors*, Technology & Engineering, CRC Press, 173 (2007) New York.
[25] M. F. Al-Mudhaffer, M. J. Griffith, K. Feron, N. C. Nicolaidis, N. A. Cooling, X. Zhou, J. Holdsworth, W. J. Belcher, and P. C. Dastoor, "The origin of performance limitations in miniemulsion nanoparticulate organic photovoltaic devices," Sol. Energy Mater. Sol. Cells **175**, 77–88, https://doi.org/10.1016/j.solmat.2017.09.007 (2018).
[26] G. F. Burkhard, E. T. Hoke, S. R. Scully, and M. D. McGehee, "Incomplete exciton harvesting from fullerenes in bulk heterojunction solar cells," Nano Lett. **9**, 4037–41 (2009).
[27] F. Nehm, T. Pfeiffelmann, F. Dollinger, L. Müller-Meskamp, and K. Leo, "Influence of aging climate and cathode adhesion on organic solar cell stability," Sol. Energy Mater. Sol. Cells **168**, 1–7 (2017).
[28] O. Pellegrino, M. Rei Vilar, G. Horowitz, F. Koiki, F. Garnier, J. D. Lopes da Silva, and A. M. Bothelho do Rego, "Characterization of oligothiophene films by high resolution electron energy loss spectroscopy," Thin Solid Films **327-329**, 252–255 (1998).
[29] H. Huang, "Studies on the electrochemistry and applications of conducting polymers," Master Thesis, 1998, Memorial University of Newfoundland, Canada.
[30] T. Liu, X. Xue, L. Huo, X. Sun, Q. An, F. Zhang, T. P. Russel, F. Liu, and Y. Sun, "Highly efficient parallel-like ternary organic solar cells," Chem. Mater. **29**, 2914–2920 (2017).